Observation of magnetic-field-induced semimetal-semiconductor transitions in crossed-gap superlattices by cyclotron resonance

D. J. Barnes*

Institute for Solid State Physics, University of Tokyo, Roppongi, Minato-ku, Tokyo 106, Japan

R. J. Nicholas

Physics Department, Oxford University, Clarendon Laboratory, Parks Road, Oxford OX1 3PU, United Kingdom
and Institute for Solid State Physics, University of Tokyo, Roppongi, Minato-ku, Tokyo 106, Japan

R. J. Warburton,* N. J. Mason, and P. J. Walker

Physics Department, Oxford University, Clarendon Laboratory, Parks Road, Oxford OX1 3PU, United Kingdom

N. Miura

Institute for Solid State Physics, University of Tokyo, Roppongi, Minato-ku, Tokyo 106, Japan

A transition from semimetallic to semiconducting behavior induced by a magnetic field has been observed in type-II superlattices of InAs/Ga$_{1-x}$In$_x$Sb by the use of very high magnetic fields, in excess of 100 T. The carrier densities and effective masses were measured by the study of cyclotron resonance using wavelengths in the region 10.6–3.39 μm. This was used to demonstrate that the zero-point energy associated with the lowest-electron and highest-hole Landau levels was sufficient to uncross the energy bands in long-period, semimetallic structures. For (100)-oriented structures this transition was found to occur in the region of 50–60 T, while for (111)A-oriented samples the uncrossing field was found to move up to the region of 100 T, due to an orientational dependence of the band offset. The effective masses, studied as a function of both photon energy and superlattice period, were found to be in good agreement with the predictions of k·p theory.

I. INTRODUCTION

Heterostructures based on the materials system InAs/GaSb are well known for the unusual property that the conduction band of the InAs lies beneath the valence-band energy of the GaSb.[1,2] The "band overlap" of the InAs conduction band and the GaSb valence band results in charge transfer across the interface until the resulting band bending equalizes the Fermi level within the structure. As a result, a wholly intrinsic system of coexisting holes and electrons, spatially separated by the interfaces, is created. The intrinsic origin of the carriers makes the system extremely sensitive to mechanisms which change the energy of the electron and hole levels such as quantum confinement and Landau level dispersion in the presence of a magnetic field.

The effects of quantum confinement can be clearly seen in superlattices of InAs/GaSb. In a superlattice structure, the electron and hole energies are raised above the band edges by the "confinement energies" which increase in value as the well width decreases. In InAs the mass of the electron is light ($m_0^* = 0.023m_e$), so that the electron confinement energy can become large in quite long-period structures. This means that the first electron level can be raised above the valence-band energy with easily achievable periodicities, thus changing the band-structure configuration from semimetallic to semiconducting. As the carriers are primarily generated because of the band overlap, a dramatic, and almost total, depopulation of the

structure accompanies this transition. The zero band-gap condition has been calculated[1,2] to occur for a superlattice periodicity of ~170 Å (85 Å InAs), although it should be remembered that since the dominant effect is the electron confinement, it is the InAs thickness that is most significant in determining this condition for superlattices with a variable InAs/GaSb thickness ratio.

The semimetal-to-semiconductor transition can also be induced magnetically.[3] The application of a magnetic field perpendicular to the layers causes the formation of Landau levels fanning upward in energy from the electrons and downward in energy from the holes. If the superlattice already has a positive band gap (semiconducting behavior due to a short periodicity) then the resulting behavior is quite straightforward. If, however, the superlattice has a negative band gap (semimetallic) then the Landau levels overlap and strong mixing and anticrossing between the conduction and valence bands occurs.[4] Nevertheless, at sufficiently high magnetic fields the lowest-electron and highest-hole levels uncross, and the energy spectrum becomes similar to that of a semiconductor. Detailed calculations demonstrate that for a superlattice with a negative band gap of order $E_g = 0.08$ eV the semimetal-to-semiconductor transition occurs at roughly 36 T.[5] In this paper we demonstrate the observation of this magnetic-field-induced semimetal-to-semiconductor transition through the observation of a rapid and dramatic fall in the carrier densities at high fields, and use this to show that in some structures over 95% of the electrons present at low field result from intrinsic charge transfer.

There have been many transport and far-infrared studies performed on both semimetallic and semiconducting InAs/GaSb superlattices. Simple Hall measurements[6] and later two-carrier fits to Hall measurements[7,8] have demonstrated the semimetal-to-semiconductor transition due to subband confinement, while cyclotron resonance (CR) data have exploited the strong nonparabolicity of InAs to confirm the presence of well developed superlattice subbands which raise the electron mass well above the band-edge value.[9] Moreover, low magnetic-field CR studies have observed complex data in multiply populated subbands, which have been interpreted as due to both interband (i.e., electron to hole) resonances as well as the expected intralevel electron cyclotron resonance.[10-12] Both interband[13] and magnetotransport experiments[14,15] have also been used to demonstrate a hydrostatic pressure-induced semimetal-to-semiconductor transition.

Here we report cyclotron resonance measurements at magnetic fields of up to 150 T, generated using a destructive single-turn coil technique. Cyclotron resonance is the ideal probe for this study, as it provides a contactless method of simultaneously measuring the effective mass and carrier concentration through the resonance position and absorption strengths, respectively. Due to the large difference between the effective masses of the electron and the holes ($m^* = 0.1, 0.2 m_e$), and the cyclotron energies used, only the electron cyclotron resonance has been observed within the magnetic field accessible with this system.

We have studied a series of multiple quantum well structures based on both InAs/GaSb, and InAs/Ga$_{1-x}$In$_x$Sb, including structures grown in both [100] and [111]A substrate directions, and with a range of periods covering both semimetallic and semiconducting behavior at zero field. The magnetically induced transition to semiconducting behavior has been measured in a series of such structures, and is related to the band offsets and quantization energies in these structures.

II. SAMPLE DETAILS

Two series of InAs/GaSb and InAs/Ga$_{1-x}$In$_x$Sb superlattices have been grown by atmospheric pressure MOVPE at Oxford University. The samples consisted of 20–100 periods of the superlattice, grown on semi-insulating GaAs substrates with a 2-μm-thick buffer layer of GaSb, which was found to be sufficient to accommodate the majority of the misfit dislocations arising from the strain at the substrate-GaSb interface. The gas switching at the interface between the InAs and GaSb layers was instantaneous which is thought to favor the formation of an InSb monolayer interface,[16] whose presence has been detected by Raman scattering.[17] Early structures of this system grown by molecular beam epitaxy[5-11] (MBE) did not possess very large intrinsically generated electron and hole densities (only about 25% of the total), due to the presence of interfacial defects and the type of structures grown. Recent advances through the use of MOVPE have demonstrated much greater intrinsic contributions to the carrier densities.

A variety of different InAs/GaSb superlattices was grown with periodicities covering the range between 60 and 600 Å. As short-period superlattices are known to have low carrier concentrations a larger number of layers was grown for these superlattices to enhance the total absorption—which would otherwise have been problematically small. The superlattices were grown simultaneously onto two substrate orientations (001) and (111)A. The (111)A superlattices are of great interest because they are piezoelectrically active, and so the small strain (0.6%) which occurs in InAs/GaSb structures induces a strong electric field which acts to increase the band overlap. Moreover, it has also recently been shown by Symons et al.[18] from fits of Hall data which give the electron and hole densities, that the band overlap is larger for (111)A. For both of these reasons the (111)A superlattices show higher carrier concentrations than the equivalent (100) samples.

TABLE I. Sample characteristics. Thickness measured by TEM except values indicated by an asterisk are estimated from total thickness measurements and growth rates.

Sample	Number of periods	Thicknesses (InAs/GaSb, Ga$_{1-x}$In$_x$Sb) (Å) [100]	[111]A
		InAs/GaSb superlattices	
1131	20	300/300*	250/400*
1134	20	85/190*	85/190*
1207	100	45/45*	50/50*
1208	100	45/35*	50/35*
1209	100	30/30*	33/33*
1249	20	216/119	178/124
1252	100	103/58	110/120
1253	100	64/32	66/33
		InAs/Ga$_{0.9}$In$_{0.1}$Sb superlattices	
1263	20	450/100*	340/160*
1265	20	446/107	337/164
1266	20	450/100*	340/160*

The sample details and electrical characteristics are shown in Table I. The superlattice periods were measured by both interference fringes observed in infrared reflectivity and transmission electron microscopy (TEM), and the individual layer thicknesses were estimated from the bulk growth rates and TEM characterization. In some cases it was found that (001) and (111)A substrates led to substantially different growth rates for the two different layers. The majority of the structures were grown with a ratio of InAs to GaSb layer thicknesses of order 3:2, in an attempt to enhance the relative proportion of holes present. For structures which show large semimetallic carrier concentrations the total electron and hole concentrations were measured using a two-carrier fit to the magnetoresistance and Hall voltage. Measurements of Shubnikov–de Haas oscillations and quantum Hall effect show that usually all layers in the superlattice are electrically active.[18]

Three superlattices of InAs/(Ga$_{1-x}$In$_x$)Sb ($x = 10\%$) were also grown and studied, but using a considerably larger thickness ratio of 5:1 for the InAs:(Ga$_{1-x}$In$_x$)Sb. The addition of 10% In into the GaSb has the effect of decreasing its band gap, and studies of GaSb/(Ga$_{1-x}$In$_x$)Sb quantum wells[19,20] suggest a band offset ratio for this system of $Q_c = \Delta E_c / \Delta E_g = 0.5$. For $x = 0.1$ the band gap of the (Ga$_{1-x}$In$_x$)Sb alloy has decreased by approximately 60 meV, and thus the band overlap of a type-II superlattice with this alloy composition can be expected to increase by of order 30 meV. The increased lattice mismatch also causes the strain to increase to of order 1%, which is expected to be particularly significant for the [111]A samples.

III. EXPERIMENTAL TECHNIQUES

The ultrahigh magnetic fields used for the experiments reported in this paper were generated using a destructive single-turn coil technique at the MegaGauss Laboratory, University of Tokyo. A 5-μsec single pulse was generated by the fast discharge of a 100 kJ, 40 kV capacitor bank across a copper single-turn coil. The peak value of the field could be increased by decreasing the diameter of the coil, 12 mm producing a peak field of 130 T, 10 mm producing 150 T, etc. As the field-time profile is roughly sinusoidal, the resolution across the resonance was maximized by choosing a coil size so that the peak magnetic field was fairly close to the resonance. It should be emphasized that despite the destruction of the coil during the pulse, all explosive forces are contained, and the sample remains unharmed, thus allowing the same piece of material to be used for repeated measurements.

The sample was held in place and cooled to 30 K by a phenol continuous flow cryostat carrying liquid helium. The transmitted radiation was detected by a fast response HgCdTe detector cooled to liquid-nitrogen temperatures. Embedded in the cryostat is a pickup coil capable of measuring the magnetic field to better than 2%. The signals from both the pickup coil and the detector were transmitted via optical fiber to a fast-acting transient recorder.

Two lasers were used for taking the majority of the

data reported in this paper, a CO$_2$ laser capable of generating a range of wavelengths around 9–10 μm, and a CO laser operating around 5 μm. Some trial experiments were also performed using a 3.39 μm He-Ne laser. In all cases the lasers were used in continuous mode, with a 100:1 mark space ratio chopper to reduce the sample heat load. Typical laser intensities at the sample were of order 5 W/cm^2 and are not thought to cause significant sample or electron heating. A more thorough description of the single-turn coil magnet and its adaptation for optical measurements can be found in Nakao *et al.*[21]

IV. EXPERIMENTAL RESULTS

A. Superlattice period effects

Cyclotron resonance was performed for the full range of structures as shown in Table I for both substrate orientations, at wavelengths of 10.61 and 9.26 μm (116 and 133 meV). The results follow a general trend typified by the series of recordings in Fig. 1, which shows the resonances for three samples of progressively decreasing period, grown on (100) GaAs, taken using 9.26 μm.

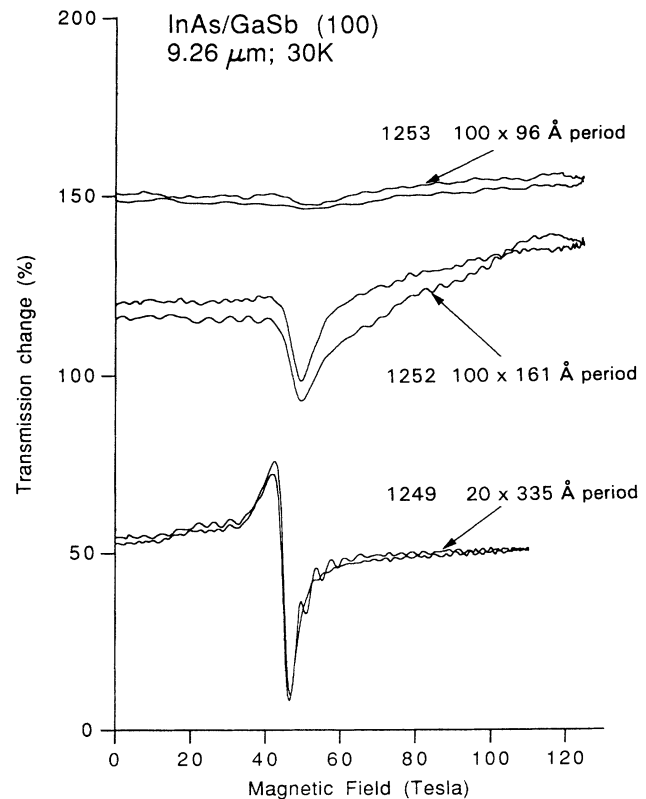Probably the most striking aspect of the data is their

FIG. 1. Experimental traces of the transmission of 9.26-μm radiation through several of the samples grown on (100)-oriented substrates, with details given in Table I. The traces show two lines, measured on the up and down sweep of the pulsed magnetic field, and demonstrate the good reproducibility of the data. The sample temperature is 30 K. The curves are offset for clarity.

simplicity—each measurement resulted in a single strong resonance, corresponding to the electrons, which are located primarily in the InAs layers. This is in obvious contrast with previous studies at lower fields, in which complex multiresonance features were observed (Guldner et al.,[10] Maan and co-workers,[11,12] and Claessen and co-workers[13,22]). At the high laser energies used here the frequencies are well above both the optical phonons and the equivalent three-dimensional plasma frequency, which makes the interpretation considerably simpler. The relatively heavy mass of the holes [~0.1 and $0.2m_e$ (Refs. 23 and 24)] puts their resonances at substantially higher fields which are above the semimetal-to-semiconductor transition and beyond the maximum magnetic field.

The long-period superlattices exhibit narrow and strong electron resonances which become weaker and broader and move up in magnetic field as the periodicity decreases, until at very short periods (<85 Å) the resonances disappear entirely. (When comparing the resonant absorptions, it should be noted that the shorter period superlattices have more layers to increase the total absorption.) In some of the longer period structures the

contribution to the dielectric function is so strong and rapidly varying that very pronounced interference effects are observed, leading to distorted resonances, as seen for the 336-Å period structure. This could not be avoided by the normal process of substrate wedging, since the interference mainly takes place within the superlattice and buffer layers due to the rather short wavelengths used in this study.

As the integrated absorption area of a resonance is related to the total carrier concentration present, the collapse of the cyclotron resonance with decreasing period can be directly ascribed to the semimetal-to-semiconductor transition. In long-period superlattices, the charge transfer across the interfaces leads to a series of high-density electron gases which, because of the resultant strong band bending are almost isolated and essentially two dimensional. Such structures possess high mobilities, and thus narrow cyclotron resonances due to weak interface scattering and strong screening. As the period decreases, however, the cyclotron resonance broadens and the absorption decreases. Here, the increasing confinement energies are acting to decrease the band overlap, resulting in a reduced carrier concentration. The smaller well width increases the importance of scattering from the interfaces, which are thought to be significant sources of charged defect states, and also the effect of layer width fluctuations which are seen to be proportionately larger in TEM images of the shorter period structures. For the shortest periods the carrier densities are found to be small, corresponding to the doping levels found in the equivalent bulk materials, of order 3×10^{16} cm^{-3}.

A similar series of resonances is shown in Fig. 2, for the equivalent superlattices grown on (111)A substrates. These structures show a similar general behavior to the (100) case, however, the carrier densities are substantially larger and shorter periodicities are required to cause the crossover to semiconducting behavior. Both changes are due to an increased band overlap, the origin of which can be attributed to the effects of the piezoelectric field[25] and the larger band overlap occurring for (111)-oriented interfaces, as reported recently by Symons et al.[18] These authors deduced the band overlap by calculating the confinement energies self-consistently, fitting the carrier densities deduced to the electron and hole densities measured from Hall effect and Shubnikov–de Haas oscillations. The band overlap for (111)A was found to be enhanced to ~200 meV, in contrast to the value of ~140 meV found for (100). This was attributed to the presence of an interface dipole layer.
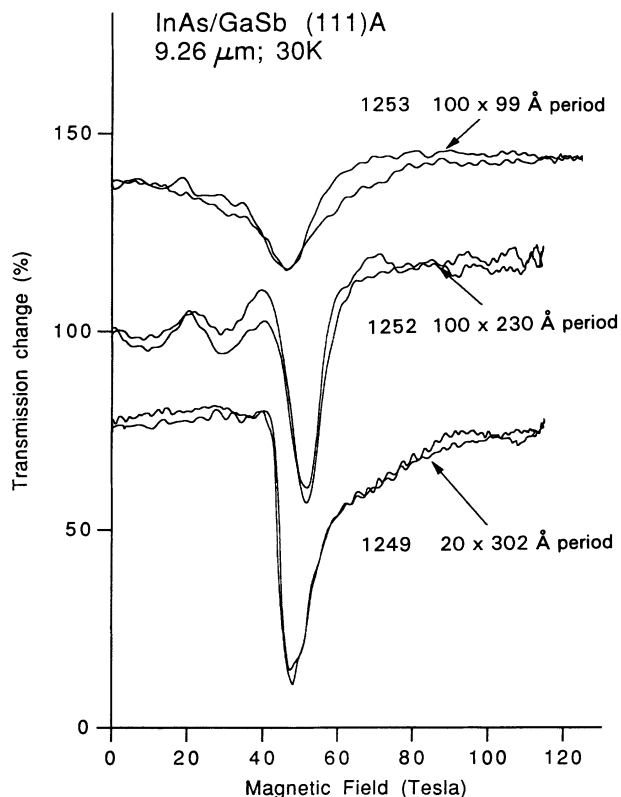

FIG. 2. Experimental traces of the transmission of 9.26-μm radiation through several of the samples grown on (111)A-oriented substrates, with details given in Table I. Substantially larger absorptions are observed than for the (100) case, shown in Fig. 1. The traces show two lines, measured on the up and down sweep of the pulsed magnetic field, and demonstrate the good reproducibility of the data. The sample temperature is 30 K. The curves are offset for clarity.

B. Magnetic-field dependence

After the general trends had been identified for the full range of possible periodicities, two samples were chosen for a closer study at fields up to 150 T. The first, 1249, is a relatively long-period semimetal, and the second, 1252 is a smaller band-gap semimetal, which is closer to the transition to semiconductor behavior. The samples selected are also notable for their high mobilities and the quality of their interfaces, as seen in TEM pictures. Cy-

clotron resonance was performed on the these superlat-
tices at wavelengths of 10.61, 9.26, 5.7, and 5.3 μm (116,
133, 216, and 233 meV, respectively).

The series for 1249 and 1252, both of which possess
large semimetallic carrier densities at low fields, are
shown in Fig. 3. The longer period superlattice exhibits
strong cyclotron resonance indicative of a high carrier
concentration sample. The resonances at 40 and 50 T are
heavily distorted due to interference, making an accurate
measurement of the exact carrier density difficult, howev-
er, the absorption intensity is estimated by using the total
swing of the transmission on passing through the reso-
nance. This is found to give reasonable agreement with
the densities measured from low-field Hall measurements,
but can only be regarded as an estimate rather than a pre-
cise measurement. However, even with this complica-
tion, it can be clearly seen that the resonance intensity
has fallen dramatically when the resonance field has
moved up to 100 T, leaving only a weak absorption
feature due to extrinsic carriers. This dramatic decrease
in the carrier density is the result of the rising zero-point
energy of the lowest electron and hole Landau levels,
which uncrosses the band overlap. At this point, the
band alignment changes from being semimetallic to semi-
conducting and the superlattice depopulates. The same
effect is seen in 1252, however, the increased quantum
confinement energies in this structure, due to the lower
period, results in both a lower density and a more rapid
depopulation at lower fields, as seen by the weaker reso-
nances and large decrease in strength between the traces
taken using 10.61 and 9.26 μm at 40 and 50 T.

The fall in carrier density is shown quantitatively as a
function of field in Fig. 4, with the carrier densities per
layer estimated from the classical absorption intensity as
described above, and the low-field data taken from the
Hall-effect measurements. The systematic field depen-
dence is not very precise due to the limited number of
field values used, however, we can estimate the field when
the carrier densities are halved to be in the region of 60

and 45 T for 1249 and 1252, respectively. The very low
densities deduced for the high fields ($\sim$ 100 T) demon-
strate the intrinsic origin of the overwhelming majority of
the carriers in these structures, with around 90% of the
carriers present at low field due to intrinsic charge
transfer. This is in strong contrast to the values found in
the structures grown earlier by MBE,[6-12] in which only
$\sim$ 25% of the carriers were of intrinsic origin.

A quantitative calculation of the magnetic-field depen-
dence of the lower Landau levels is shown in Fig. 5, cal-
culated using an eight-band k·p perturbation theory,[26]
for the zone-center (Γ point) miniband edge. The model
includes coupling between the conduction, valence, and
spin-orbit splitoff bands, and is performed using the axial
approximation using a numerical procedure to implement
the boundary conditions at the superlattice interfaces, but
ignoring any Bloch function mixing.[27] The model is only
qualitative, as it does not include the full self-consistent
superlattice potential resulting from the charge transfer
and the resultant band bending. Instead the relative
thicknesses of the InAs and GaSb are adjusted to match
the valence subband—conduction subband overlap cal-
culated from the low-field electron and hole densities.
The calculation shown is for a band gap of -77 meV and
predicts that the uncrossing should occur at magnetic
fields in the region of 36 T, as indicated by the vertical
dashed line. This is consistent with the experimental
data. The depopulation of the superlattice which marks
the band uncrossing can be seen very clearly in the data
for 1252 (001), when the resonance field increases from 40
to 50 T. Sample 1249, which has the longest periods and
thus has the most negative band gap, requires the highest
magnetic field to cause the band uncrossing.

An interesting feature of the calculations is the forma-
tion of an energy gap, at low magnetic fields, due to the
interaction of the Landau levels of the electrons and
holes, as noted for this system by Fasolino and Altarelli.[28]
By contrast the lowest-electron and highest-hole levels do
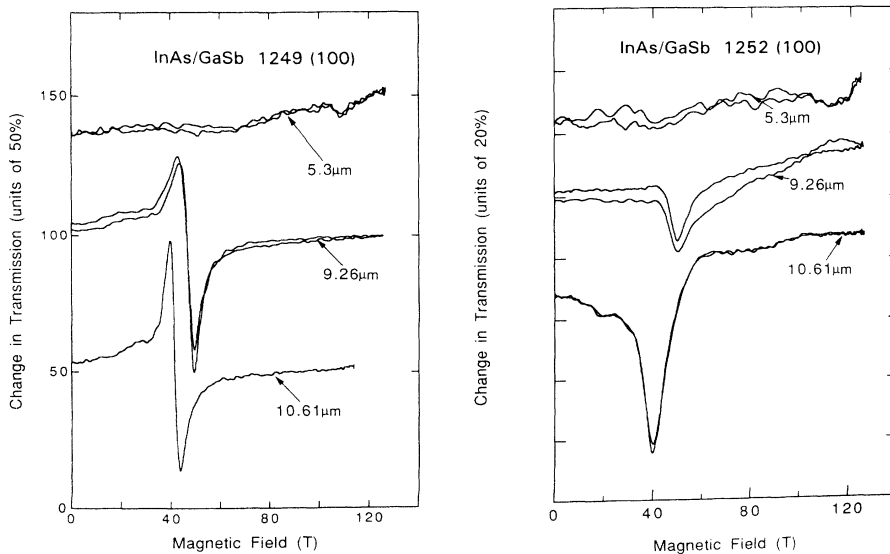not mix and there is no anticrossing behavior, due to

FIG. 3. Experimental absorp-
tion traces at 10.61, 9.26, and 5.3
μm for two (100)-oriented sam-
ples at 30 K. The traces are
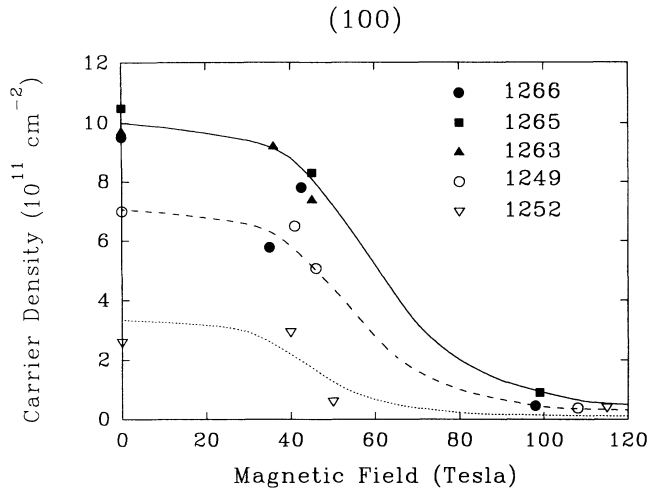offset for clarity.

(100)

FIG. 4. A plot of the carrier density as a function of magnetic field for five of the (100) samples studied in detail, as deduced from the absorption strengths and the low-field Hall effect. The lines shown are a guide to the eye, but all have the same functional form and are scaled in magnetic field by factors of 1, 0.9, and 0.75.

their different axial quantum numbers. Some mixing may be expected in reality, due to both the nonaxial nature of the full anisotropic Luttinger Hamiltonian, and possible Bloch function mixing effects.[27]

It is also clear from the fits that it is likely that we should expect to see interband transitions above the semimetal-to-semiconductor transition, particularly that from the uppermost hole level to the lowest-electron level at high fields, in the region of 60–100 T. There is some evidence for a weak transition, in the very small absorption visible in the region of 100 T for sample 1252, in Fig. 3, but only a relatively weak absorption is to be expected due to the type-II band alignment and the relatively long superlattice period, which leads to only small wavefunction penetration from one layer to the next. A candidate for this type of transition, however, is the very small absorption visible in the region of 100 T for sample 1252, seen in Fig. 3.

Similar measurements were made for the (111)A-oriented structures, shown in Fig. 6, which exhibit several important differences from the (100) structures: The carrier densities are substantially higher than for (100) as described above, and significant depopulation is still occurring in the region above 100 T. A plot of carrier density as a function of magnetic field in Fig. 7 shows these effects qualitatively. Again the identification of a precise field position associated with the uncrossing of the lowest Landau levels is difficult, however, it is clear that the field required to halve the carrier density has now moved up to the region of 100 T. This is consistent with the suggestion of an additional band overlap of ~60–70 meV for (111) made by Symons et al.,[18] and discussed above.

The influence of this additional band overlap has been included in the eight-band k·p calculations by the addition of 70 meV for the band offsets, and the calculations

have been repeated, using the appropriate changes to the Hamiltonian. The Landau levels for the (111) case calculated in this way are also shown in Fig. 5. The level diagram is considerably more complex, due to the larger
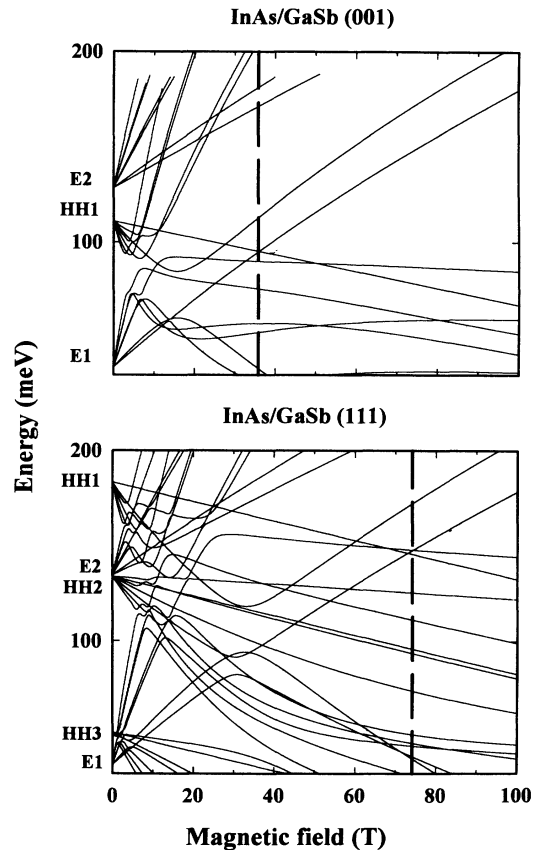

FIG. 5. The theoretically calculated Landau levels of a 200 Å InAs/50 Å GaSb superlattice, as a function of magnetic field, ignoring all Coulomb contributions to the potential. The calculation uses a full solution of the eight-band k·p Hamiltonian, and demonstrates the importance of strong mixing between the conduction- and valence-band energy levels. The results shown in the upper section are based on the assumption of a band-edge overlap of 140 meV, appropriate to the (100) case. The strong dashed line shows the magnetic field at which the lowest-electron level and the highest-hole level cross, corresponding to the semimetal-to-semiconductor transition. The results for the lower curves are calculated with the Luttinger Hamiltonian appropriate for the (111) orientation, and use a band overlap of 200 meV, which is thought to have been increased over the value for (100) due to the presence of an interface dipole. The calculations use the axial approximation, in which a good quantum number n can be defined which, in the standard nomenclature runs from $n = -2, -1, 0, 1, \ldots$ (Ref. 26). When the valence-conduction band coupling is weak, for instance well above the semimetal-semiconductor transition, there is an $n = 1$ hole level with $m_J = +\frac{3}{2}$, $n_{LL} = 0$ character, an $n = 0$ electron level with $m_z = +\frac{1}{2}$, $n_{LL} = 0$, and an $n = -1$ electron level with $m_J = -\frac{1}{2}$, $n_{LL} = 0$, where n_{LL} is the conventional Landau level index. The $n = -2$ state gives a pure hole $m_J = -\frac{3}{2}$, $n_{LL} = 0$ level for all fields. These are the four levels which can be seen to cross near the strong dashed lines in the figures. In each figure, quantum numbers $n = -2$ to 2 are plotted, and the energy scale is measured from the InAs conduction-band edge.
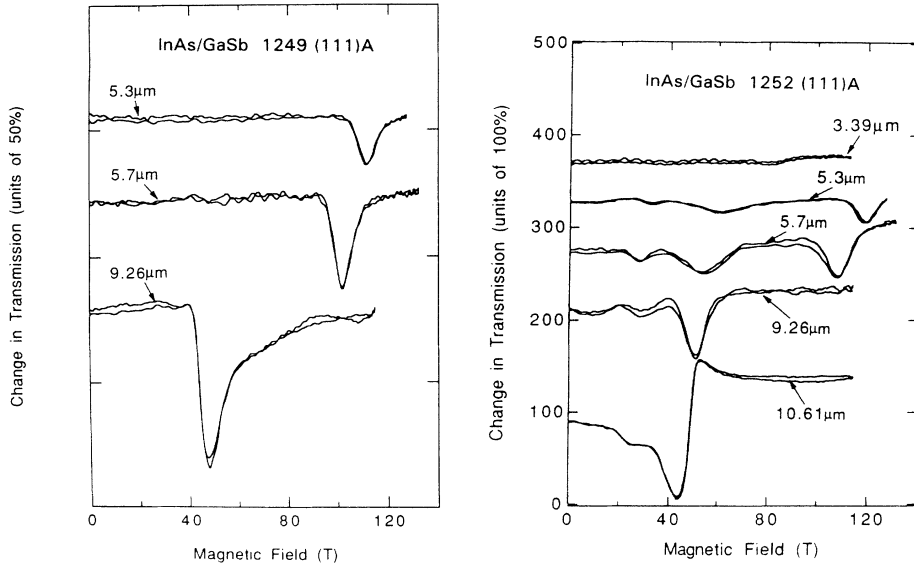
FIG. 6. Experimental absorption traces at 10.61, 9.26, 5.7, 5.3, and 3.39 μm for two (111)A-oriented superlattices. The data are taken at 30 K and the traces are offset for clarity. It is obvious that a number of additional resonances occur for 1252 (111)A.

number of confined subbands which are overlapping, a factor which is increased due to the heavier hole mass for the (111) orientation. The calculation predicts that the band uncrossing increases from the (100) value of $\sim$40 to $\sim$75 T, which is in agreement with the experimental conclusions from comparing the data of Figs. 4 and 7.

In addition, an unexpected feature of the data for 1252 (111) is the appearance of a series of new resonances at low fields. These occur at fields approximately $\frac{1}{2}$ and $\frac{1}{4}$ of the fundamental cyclotron resonance, and increase in strength as the wavelength decreases and the resonances move to higher fields. This corresponds to the excitation of cyclotron resonance harmonics. A detailed discussion of these transitions will be given in Sec. V, describing the resonance positions and effective masses, where it will be

seen that they correspond in practice to spin-flip resonances given, to a first approximation, by the energy $2\hbar\omega_c - g_{\mu B}B$, which are allowed by mixing with the valence band. These resonances are particularly strong in the region where the Landau states of the lowest-electron Landau level are crossing the valence band. For the one case of the sample 1252 (111)A, the studies were extended to still higher energies using the 3.39-μm radiation from a HeNe laser. This trace is also shown in Fig. 6. The strong nonparabolicity of the electron levels puts the fundamental resonance for an energy of 345 meV at around 190 T, well above the maximum magnetic field available, however, weak low-field structure can be seen. Two resonances were observed at relatively low fields close to the $N=4$ and 6 harmonics, with a weaker feature around $N=3$. The strength of the $N=3$ harmonic in comparison to the results for longer wavelengths is not yet understood.
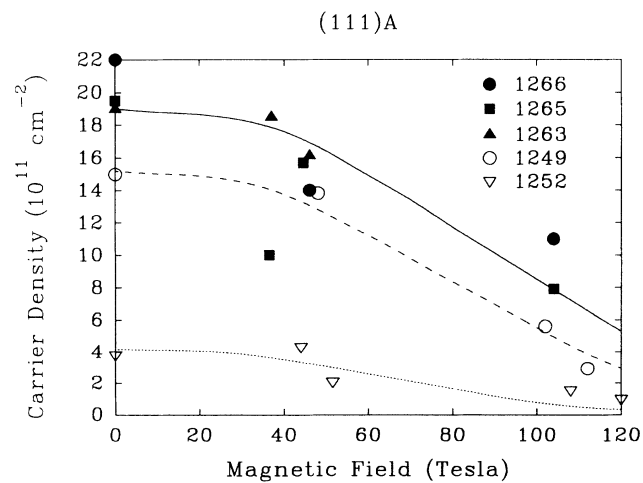
C. InAs/Ga$_{1-x}$In$_x$Sb superlattices

Cyclotron resonance was also performed on three InAs/Ga$_{1-x}$In$_x$Sb superlattices of roughly the same dimensions at 10.61, 9.26, and 5.5 μm. In this series of structures the Ga$_{1-x}$In$_x$Sb layer thicknesses were $\sim$100 Å, with x values of 0.1, leading to a substantial additional strain of order 1% and with much thicker InAs layers of 500 Å. For the case of InAs/Ga$_{1-x}$In$_x$Sb superlattices there will be an additional band overlap of order 30 meV, as estimated from GaSb/Ga$_{1-x}$In$_x$Sb quantum well structures,[16,17] due to the additional shift upwards of the Ga$_{1-x}$In$_x$Sb valence-band edge, with reference to the GaSb valence-band edge. Also noteworthy is that the low-field Hall traces for these structures indicated that the ratio of electrons to holes in these structures was close to 1:1.

The cyclotron resonance traces are shown in Fig. 8, for both (100) and (111)A orientations. The behavior seen is very similar to that for 1249 InAs/GaSb, but the resonances show substantially less distortion. At low magnet-

FIG. 7. A plot of the carrier density as a function of magnetic field for five of the (111)A samples studied in detail, as deduced from the absorption strengths and the low-field Hall effect. The lines shown are a guide to the eye, but all have the same functional form and are scaled in magnetic field by factors of 1, 0.95, and 0.75.

ic fields around 40 T there is a strong symmetric absorption, with a higher intensity for $(111)A$ than (100). There are also weak indications of two additional resonances just above and below the main absorption for the data at 9.2 and 10.6 μm for $(111)A$. At high fields, around 100 T, the behavior of the two orientations is very different—the (100) superlattices are totally depopulated while the $(111)A$ structures are only $\sim 50\%$ reduced—reflecting a significantly larger band overlap for the (111) orientation as expected. In agreement with the low-field Hall data these results show that the (100) superlattices are of order 95% intrinsic.

The magnetic-field dependence of the carrier densities for these superlattices are also included in Figs. 4 and 7 for the (100) and (111) orientations, respectively, which show that the qualitative dependences are very similar to those seen for the InAs/GaSb structures. The larger band overlap and the wider InAs layer thicknesses for the InAs/Ga$_{1-x}$In$_x$Sb superlattices result in higher carrier concentrations and transition fields than for the accompanying InAs/GaSb data. For the (100)
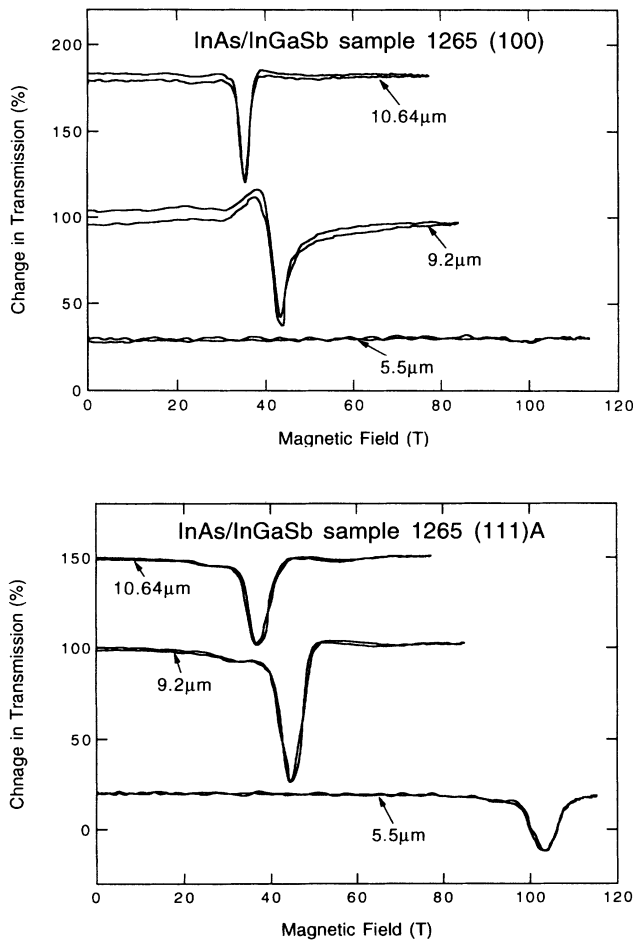
InAs/Ga$_{1-x}$In$_x$Sb superlattices the transition field is increased to about 60 T, as is predicted by the same eight-band k·p calculation as described above. In this case the zero-field band overlap is found to be 96 meV, taking into account the additional overlap of the InAs/Ga$_{1-x}$In$_x$Sb superlattices which results from the shift of the band edges and the presence of a larger strain component,[29] and the somewhat different confinement energies for the electrons and holes. For the (111) InAs/Ga$_{1-x}$In$_x$Sb superlattices the semiconductor-to-semimetal transition is shifted up in field to the region of 100 T, consistent with a larger band overlap for this orientation.

V. EFFECTIVE MASSES

The cyclotron resonance positions have been used to examine the dependence of the effective mass on both energy and superlattice period. Figure 9 shows a plot of the effective masses as a function of energy for both an InAs/GaSb and an InAs/Ga$_{1-x}$In$_x$Sb superlattice for both (100) and (111) orientations. The effective mass is found to be given to a good approximation by the linear dependence:

$$m^* = m^*_{\mathrm{SL}}[1 + 2.6\hbar\omega_c/(E_g + E_{\mathrm{conf}})] , \qquad (1)$$

which is the functional form expected for a simple two-band nonparabolic approximation for the effective mass, where $\hbar\omega_c$ is the cyclotron energy and E_g is the bulk InAs band gap, but with an increased value to the energy prefactor as has been found previously from results in a number of different III-V materials.[30,31] E_{conf} is the

FIG. 8. Experimental traces for both (100)- and (111)-oriented samples of the InAs/Ga$_{1-x}$In$_x$Sb sample 1265 taken at 10.61, 9.26, and 5.5 μm at 30 K. The traces are offset for clarity, and demonstrate the almost total disappearance of the resonance at 100 T for the (100) sample.
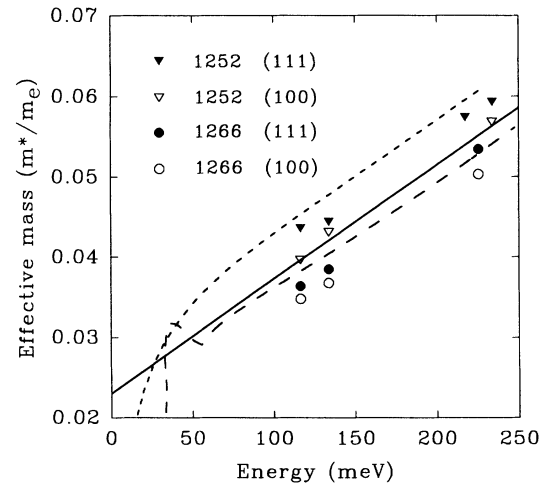

FIG. 9. Plots of the energy dependence of the effective mass measured for two of the superlattices for (100) and $(111)A$ orientations. The solid line shows a fit to the linear approximation given in Eq. (1), with $m^*_{\mathrm{SL}} = 0.024$ and $E_{\mathrm{conf}} = 30$ meV. The short and long and dashed lines show the results of the effective mass as deduced from the calculations described in the text, using superlattice layer thicknesses of 85 Å/50 Å (short dashed lines) and 200 Å/50 Å (long dashed lines). The sharp anomalies at low energies are the result of level crossing effects.

D. J. BARNES *et al.*

confinement energy due to the superlattice potential. The value of the band-edge mass m_{SL}^* was sample dependent, and will be discussed below. The agreement between this linear dependence and the experiment suggests that the electron behavior is dominated by the InAs in which the electron wave function is primarily located. For a better fit, the effects from higher bands must be included in the calculation. This is shown using the results of the detailed eight-band k·p theory, calculated for two different structures with InAs/GaSb thicknesses of 200 Å/50 Å and 85 Å/50 Å, which correspond to zero-field band gaps of -0.077 and 0 eV. These provide a good description of the observed behavior, and at high fields give very similar results to the linear form.

The effective mass values for the InAs/Ga$_{1-x}$In$_x$Sb superlattices are slightly lower than those of the InAs/GaSb structures due to the larger InAs thicknesses, which lead to lower confinement energies. The $(111)A$ structures have a slightly higher mass, due to the larger confinement energies which result from the stronger self-consistent confinement potential caused by the higher carrier densities for this orientation. A similar linear increase in effective mass with energy has been observed in single quantum wells of InAs in AlSb, by Yang *et al.*,[32] who found that there was also a significant decrease in the band-edge effective-mass value due to the tensile strain present in InAs wells grown at the lattice constant of GaSb. This factor will be less significant for the structures studied here, since the large total superlattice thickness leads to the formation of essentially free standing "strain braced" structures.

A further conclusion from the detailed k·p calculations is that the field positions of the harmonic resonances can be accurately predicted by the assignment of the transitions to a change in axial quantum number of three units. In the description of the Landau levels as unperturbed states, these correspond to spin-flip resonances in which the spin is flipped simultaneously with excitation between two Landau levels, giving a transition at an energy of $2\hbar\omega_c - g_{\mu B}B$. This process is allowed due to the interaction between the conduction band levels, originating primarily in the InAs, and the valence bands in the GaSb. It is not at present clear why this behavior should be so much more pronounced in one particular (111) sample; however, there are weak indications of further resonances for other samples, such as 1249 (100) at 5 μm, and 1265 $(111)A$ at 9.2 μm and 10.6 μm. This suggests that the harmonic transitions may be enhanced by particular level degeneracies or crossings which occur for specific structures at particular fields. In addition the full Luttinger Hamiltonian for (111) contains several additional off-diagonal terms which will mix states of different axial quantum number and thus enhance the probability of higher angular momentum transfer transitions.

The only previous reports of the observation of cyclotron resonance harmonics were those observed in silicon metal-oxide-semiconductor structures[33] which were attributed to the presence of strong electron-electron interactions. In contrast with the present measurements, these authors observed the complete set of harmonics, which leads us to believe that the present observations have a
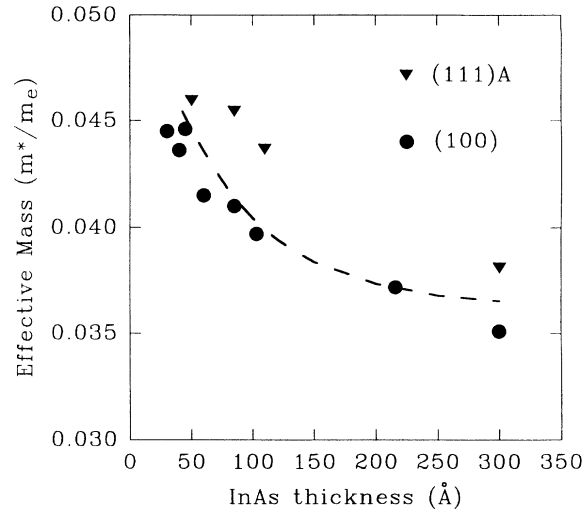

FIG. 10. Plots of the effective mass measured at 115 meV (10.61 μm) as a function InAs thickness in the series of InAs/GaSb samples. The dashed line shows the results of the simple two-band k·p formula [Eq. (2)], in which the confinement energy has been calculated by the accurate eight-band k·p theory in zero field.

different origin, as described above.

The effective mass has also been studied as a function of InAs layer thickness for a fixed laser wavelength of 10.61 μm, as shown in Fig. 10. The dependence on InAs thickness is used to plot the results in order to allow a comparison of data taken on samples with varying ratios of InAs:GaSb. The InAs thickness is more significant than the superlattice period in such structures, since the electron mass is dominated by the InAs conduction band. The systematic increase in mass as the superlattice period is decreased is due to the increasing importance of the superlattice confinement energy and nonparabolicity. The dependence of the effective mass on period was modeled using

$$m^* = m_0^* [1 + (2.6\hbar\omega_c + E_{conf})/E_g] , \qquad (2)$$

which is equivalent to Eq. (1), but with the superlattice mass generated from the band-edge mass $m_0^* = 0.021$, which is rather lower than the accepted bulk InAs value of 0.023, and values for E_{conf}, which were calculated at zero field as a function of the superlattice parameters using the eight-band k·p theory. The agreement between experiment and theory can be seen from Fig. 10 to be excellent. The difference in the influence of the confinement energy E_{conf} and the in-plane kinetic energy $(\hbar\omega_c)$ is a consequence of the decoupling of the motion in the two directions, as has been shown theoretically by Ekenberg,[34] and experimentally by Warburton *et al.*,[35] for the case of GaAs/Ga$_{1-x}$Al$_x$As quantum wells.

In conclusion we can state that we have provided clear evidence for the observation of the magnetically induced semimetal-to-semiconductor transition in a range of InAs/Ga$_{1-x}$In$_x$Sb superlattices. This has been achieved

by the use of cyclotron resonance to monitor the carrier densities as a function of magnetic field. The field position of the transition is a strong function of both the superlattice periods, due to the confinement energies, and the interface orientation. This provides strong support for the recent suggestion that the band overlap in this materials system is strongly orientation dependent.

---

*Present address: Sektion Physik, Universitat Munchen, Geschwister Scholl-Platz 1, D-8000 Munich 22, Germany.

[1]L. L. Chang, J. Phys. Soc. Jpn. **49**, Suppl. A, 997 (1980).

[2]L. Esaki and L. L. Chang, J. Magn. Magn. Mater. **11**, 208 (1979); L. L. Chang and L. Esaki, Surf. Sci. **98**, 70 (1980).

[3]N. J. Kawai, L. L. Chang, G. A. Sai-Halasz, C. A. Chang, and L. Esaki, Appl. Phys. Lett. **36**, 369 (1992).

[4]A. Fasolino and M. Altarelli, Surf. Sci. **142**, 322 (1984).

[5]D. J. Barnes, R. J. Nicholas, N. J. Mason, P. J. Walker, R. J. Warburton, and N. Miura, Physica B **184**, 168 (1993).

[6]L. L. Chang, N. Kawai, G. A. Sai-Halasz, R. Ludeke, and L. Esaki, Appl. Phys. Lett. **35**, 939 (1979).

[7]E. E. Mendez, L. Esaki, and L. L. Chang, Phys. Rev. Lett. **55**, 2216 (1985).

[8]H. Munekata, E. E. Mendez, Y. Iye, and L. Esaki, Surf. Sci. **174**, 449 (1986).

[9]H. Bluyssen, J. C. Maan, P. Wyder, L. L. Chang, and L. Esaki, Solid State Commun. **31**, 35 (1979).

[10]Y. Guldner, J. P. Vieren, P. Voisin, M. Voos, L. L. Chang, and L. Esaki, Phys. Rev. Lett. **45**, 1719 (1980).

[11]J. C. Maan, Y. Guldner, J. P. Vieren, P. Voisin, M. Voos, L. L. Chang, and L. Esaki, Solid State Commun. **39**, 683 (1981).

[12]J. C. Maan, Ch. Uhilein, L. L. Chang, and L. Esaki, Solid State Commun. **41**, 755 (1982).

[13]L. M. Claessen, J. C. Maan, M. Altarelli, P. Wyder, L. L. Chang, and L. Esaki, Phys. Rev. Lett. **57**, 2556 (1986).

[14]J. Beerens, G. Gregoris, J. C. Portal, E. E. Mendez, L. L. Chang, and L. Esaki, Phys. Rev. B **36**, 4742 (1987).

[15]R. J. Nicholas, K. S. H. Dalton, M. Lakrimi, C. Lopez, R. W. Martin, N. J. Mason, G. M. Summers, G. M. Sundaram, D. M. Symons, P. J. Walker, R. J. Warburton, M. I. Eremets, D. J. Barnes, N. Miura, L. Van Bockstal, R. Boegaerts, and F. Herlach, Physica B **184**, 268 (1993).

[16]M. Lakrimi, R. W. Martin, N. J. Mason, R. J. Nicholas, and P. J. Walker, J. Cryst. Growth **110**, 677 (1991).

[17]C. Lopez, R. J. Springett, R. J. Nicholas, P. J. Walker, N. J. Mason, and W. Hayes, Surf. Sci. **267**, 176 (1992).

[18]D. M. Symons, M. Lakrimi, R. J. Warburton, R. J. Nicholas, N. J. Mason, P. J. Walker, and M. I. Eremets, Semicond. Sci. Technol. **9**, 118 (1994).

[19]S. K. Haywood, E. T. R. Chidley, R. E. Mallard, N. J. Mason, R. J. Nicholas, P. J. Walker, and R. J. Warburton, Appl. Phys. Lett. **54**, 922 (1989).

[20]S. L. Wong, R. J. Warburton, R. J. Nicholas, N. J. Mason, and P. J. Walker, Physica B **184**, 106 (1993).

[21]K. Nakao, F. Herlach, T. Goto, S. Takeyama, T. Sakakibara, and N. Miura, J. Phys. E **18**, 1018 (1985).

[22]L. M. Claessen, J. C. Maan, M. Altarelli, P. Wyder, L. L. Chang, and L. Esaki, Superlatt. Microstruct. **2**, 551 (1986).

[23]G. M. Sundaram, R. J. Warburton, R. J. Nicholas, G. M. Summers, N. J. Mason, and P. J. Walker, Semicond. Sci. Technol. **7**, 985 (1992).

[24]M. Lakrimi, T. A. Vaughan, D. M. Symons, R. J. Nicholas, N. J. Mason, and P. J. Walker, Solid State Electron. (to be published).

[25]M. Lakrimi, C. Lopez, R. W. Martin, G. M. Summers, G. M. Sundaram, K. S. H. Dalton, N. J. Mason, R. J. Nicholas, and P. J. Walker, Surf. Sci. **263**, 575 (1992).

[26]M. H. Weiler, in *Semiconductors and Semimetals*, edited by R. K. Willardson and A. C. Beer (Academic, New York, 1981), Vol. 16, p. 119.

[27]T. Ando, S. Wakahara, and H. Akera, Phys. Rev. B **40**, 11 609 (1990).

[28]A. Fasolino and M. Altarelli, Surf. Sci. **142**, 322 (1984).

[29]C. G. Van de Walle, Phys. Rev. B **39**, 1871 (1989).

[30]M. A. Hopkins, R. J. Nicholas, W. Zawadzki, P. Pfeffer, D. Gauthier, J. C. Portal, and M. A. DiForte-Poisson, Semicond. Sci. Technol. **2**, 568 (1987).

[31]R. J. Nicholas, C. K. Sarkar, L. C. Brunel, S. Huant, J. C. Portal, M. Razeghi, J. Chevrier, J. Massies, and H. Cox, J. Phys. C **18**, L427 (1985).

[32]M. J. Yang, P. J. Lin-Chung, R. J. Wagner, J. R. Waterman, W. J. Moore, and B. V. Shanabrook, Semicond. Sci. Technol. **8**, S129 (1993).

[33]G. Abstreiter, J. P. Kotthaus, J. F. Koch, and G. Dorda, Phys. Rev. B **14**, 2480 (1976).

[34]U. Ekenberg, Phys. Rev. B **40**, 7714 (1989).

[35]R. J. Warburton, J. G. Michels, R. J. Nicholas, J. J. Harris, and C. T. Foxon, Phys. Rev. B **46**, 13 394 (1992).